

VUTH 98-17
LANCS/HEP/9806

SPIN PHYSICS IN DEEP INELASTIC SCATTERING ^a

P.J. MULDER

*Physics Department, Free University,
De Boelelaan 1081, 1081 HV Amsterdam, the Netherlands
E-mail: mulders@nat.vu.nl*

T. SLOAN

*University of Lancaster
Lancaster LA1 4YB, UK
E-mail: t.sloan@lancaster.ac.uk*

The problem of our understanding of the spin structure of the nucleon has been with us since the publication of the EMC measurements of the polarised structure function of the proton in 1987. In this talk a brief history of the subject is given followed by a review of the results presented in this workshop and the progress made to date.

1 Introduction

In the simple quark model the spin of the proton is carried by its three valence quarks so that $\Delta\Sigma = \Delta u + \Delta d = 1$. Here $\Delta q = \int_0^1 dx (q_R(x) - q_L(x))$ where $q_{R(L)}(x)$ are quark distributions for chirally righthanded (lefthanded) quarks in a polarized proton and $q = u, d$, etc. indicates the quark flavours. In a fast-moving proton the $q_{R(L)}$ are associated with quarks spinning parallel (antiparallel) to the proton helicity. The simple quark model is clearly inadequate since it predicts that the ratio of the axial vector to vector coupling constants in neutron β decay is $g_A = 5/3$ compared to the measured value of 1.26. Relativistic effects are invoked to account for this difference and correspondingly reduce $\Delta\Sigma$ to ~ 0.7 with the excess spin appearing as the effects of orbital motion.

Deep inelastic scattering (DIS) with polarised charged leptons on polarised targets allows the quark distributions $q_{R(L)}$ to be investigated. These are extracted from the structure function $g_1(x, Q^2)$ measured in polarised DIS using the parton model relation $g_1(x, Q^2) = \frac{1}{2} \sum_q e_q^2 (q_R(x) - q_L(x))$. The difference in cross sections for different orientations of the lepton and target

^aSummary talk of Spin Physics working group at the 6th International Workshop on Deep Inelastic Scattering and QCD, Brussels (1998).

nucleon polarisations are related to the polarised structure functions g_1 and g_2 by:

$$d\sigma^{\uparrow\downarrow} - d\sigma^{\uparrow\uparrow} = ag_1(x, Q^2) + bg_2(x, Q^2) \quad (1)$$

where a and b are kinematic factors calculated from QED. For parallel and antiparallel spins b is small allowing $g_1(x, Q^2)$ to be measured while if the target polarisation is perpendicular and parallel to the lepton scattering plane a is small allowing g_2 to be measured (for the exact definitions of a and b and the DIS variables x , y and Q^2 see ¹). An alternative notation uses the virtual photon asymmetries which are given by $A_1 = (\sigma_{\frac{1}{2}} - \sigma_{\frac{3}{2}})/(\sigma_{\frac{1}{2}} + \sigma_{\frac{3}{2}})$ and $A_2 = \sigma_{TL}/\sigma_T$ where $\sigma_{\frac{1}{2}(\frac{3}{2})}$ is the photoabsorption cross section in a state $J_z = \frac{1}{2}(\frac{3}{2})$ i.e. with the photon-nucleon spins antiparallel(parallel). The cross-section σ_T is the photoabsorption cross section for transverse photons and σ_{TL} is that due to the transverse-longitudinal interference. The asymmetry A_1 and g_1 are related by $A_1 = \sum_q e_q^2 (q_R(x) - q_L(x)) / \sum_q e_q^2 (q_R(x) + q_L(x)) \approx g_1/F_1$ where F_1 is the unpolarised structure function. For parallel and antiparallel lepton and nucleon spins the measured asymmetry, A_m , in any bin is related to A_1 and hence g_1 by:

$$A_m = \frac{N^{\uparrow\downarrow} - N^{\uparrow\uparrow}}{N^{\uparrow\downarrow} + N^{\uparrow\uparrow}} \approx P_B P_T f D A_1 \quad (2)$$

where P_B and P_T are the beam and target polarizations, the target dilution factor, f , is the fraction of the events from the free polarised nucleons in the target and the depolarization factor of the virtual photon D comes from QED and increases with y . The product of the factors $P_B P_T f D$ is usually small so that the asymmetries to be measured are also small.

In the early 1980s the SLAC experiments E80 and E130 ² reported the first measurements of polarised DIS for $x > 0.1$. In 1988, the EMC reported measurements ³ over a range down to $x = 0.015$. For $x > 0.1$ all the data agreed well with the expectations of the quark parton model. However, as x decreased the EMC data fell progressively below these expectations.

The significance of this disagreement with the quark parton model can be understood by examining the first moment of the proton data which the EMC measured to be

$$\Gamma_1^p = \int_0^1 g_1^p(x) dx = 0.126 \pm 0.01(stat) \pm 0.015(sys). \quad (3)$$

In the quark-parton model and to leading order in QCD this moment, for the proton and neutron, is given by

$$\Gamma_1^{p(n)} = +(-) \frac{1}{12} a_3 + \frac{1}{36} a_8 + \frac{1}{9} a_0. \quad (4)$$

Here the a_j are the diagonal combinations in the $SU(3)$ nonet of the axial matrix elements. With

$$\Delta q 2M S^\mu = \langle P, S | \bar{\psi} \gamma^\mu \gamma_5 \psi | P, S \rangle \quad (5)$$

where S^μ is the spin vector of the proton and the a_j are related to the Δq by $a_3 = g_A = \Delta u - \Delta d$, $a_8 = (\Delta u + \Delta d - 2\Delta s)$ and $a_0 = \Delta\Sigma = (\Delta u + \Delta d + \Delta s)$. The matrix elements a_3 and a_8 , measured from neutron and hyperon decay, had values of 1.254 and 0.688, respectively, at the time of the EMC measurements. Using these values and the measured value of Γ_1^p implied that $\Delta\Sigma = 0.12 \pm 0.09 \pm 0.14$ i.e. only $\sim 12\%$ of the spin of the proton is carried by its quarks.

This surprising result created great theoretical interest. Where was the spin of the nucleon? Could it be in the gluons (ΔG) as suggested in^{4,5} or could it be in orbital angular momentum (L)⁶. By angular momentum conservation the total spin of the nucleon of $1/2$ must be equal to $1/2 \Delta\Sigma + \Delta G + L$. It was also suggested that the problem did not exist and part of the measured moment was missed in a perverse Regge behaviour which caused g_1 to diverge in the unmeasured region at very small x ⁷.

All this interest created a new experimental programme to investigate the phenomenon further. At SLAC experiments E142 and E143 were done at incident polarized electron energies up to 29 GeV using polarized ^3He , hydrogenated and deuterated ammonia targets. These were followed by E154 and E155 at incident electron energies of 49 GeV using polarized targets made from ^3He , ^6Li D and hydrogenated ammonia. At DESY the HERMES experiment uses polarized gas jet targets of ^3He and atomic hydrogen. At CERN the Spin Muon Collaboration (SMC) has used hydrogenated and deuterated ammonia and butanol polarized targets with polarized muon beams of energies up to 200 GeV. Such high energies allow coverage of a wide x range. From all these experiments the structure function g_1 has been measured with much improved precision and the first measurements of the structure function g_2 have been reported. The measurements of these structure functions for the proton and neutron provide the data which will be summarized in this talk.

The data from E142 and E143¹⁰ and the early data from SMC⁹ confirmed the original EMC result³ and provided a precise and interesting check on the Bjorken sum rule¹¹. This is obtained from equation (5) by taking the difference between the first moments for the neutron and the proton so that in leading order in QCD;

$$\Gamma_1^p - \Gamma_1^n = \frac{1}{6}(\Delta u - \Delta d) = \frac{g_A}{6}. \quad (6)$$

This is a deeply fundamental sum rule which if broken implies serious conse-

quences for QCD¹². The E142 and E143 data at low $Q^2 \sim 2 \text{ GeV}^2$ ¹⁰ are shown in Fig. 1. Before QCD radiative corrections are applied the sum rule appears to be broken. However, as successive orders of QCD radiative corrections^{13 14} (see section 3) are applied the data come into agreement with the sum rule. Hence, the Bjorken sum rule appears to be playing the same part in testing QCD as $g - 2$ of the muon did for tests of QED. We look forward to future more precise tests of QCD from this sum rule.

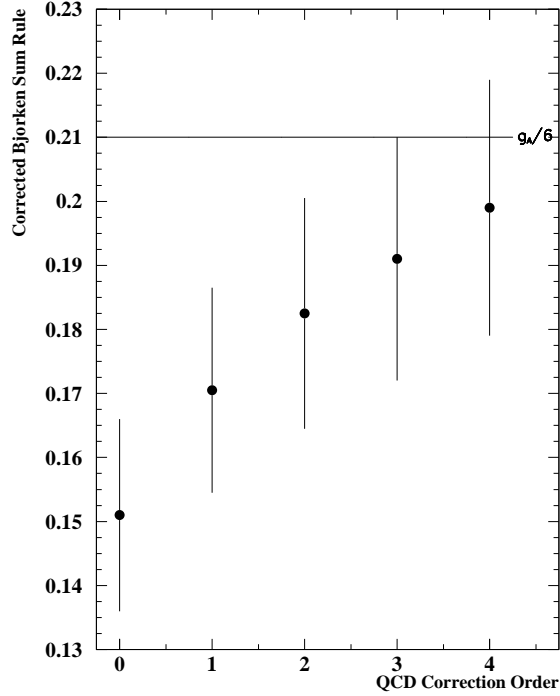


Figure 1: The value of $(\Gamma_1^p - \Gamma_1^n)/C_{NS}$ where C_{NS} is the QCD radiative correction defined in Eq. 11 as a function of the order in α_s of the calculation of C_{NS} . The values of Γ_1^p and Γ_1^n are taken from¹⁰.

2 Data Reported at DIS 98

2.1 Measurements of g_1

The SMC has presented data over the widest range of x on the polarised structure functions¹⁵. The collaboration has greatly improved the precision of the data at low x by demanding an observed hadron in each event. This rejects radiative and other events with low depolarisation factors. The remaining events are then undiluted by data of poor significance for the asymmetry determination allowing the asymmetry to be determined more precisely. Furthermore, a much lower Q^2 trigger has been implemented which allows asymmetries to be measured in the range $10^{-4} < x < 10^{-3}$. The data from this trigger serve to investigate the Regge region to search for a possible divergence at low x due to perverse behaviour such as that proposed in⁷. Fig. 2 shows the SMC data¹⁶ with the behaviour of $g_1 = 0.17/x \ln^2 x$ (solid curve) proposed by⁷. Such behaviour is excluded by the data. By implication even more extreme behaviours such as the power laws proposed in⁸ will also be excluded but direct comparison is difficult due to the uncertainties in the hardness scale. However, the less extreme behaviours $g_1 = -0.14 \ln x$ (dashed curve) and $g_1 = -0.085(2 + \ln x)$ (dotted curve) which were also proposed in⁷ cannot be excluded. All the curves were calculated assuming a value of $R = \sigma_L/\sigma_T = 0$. Hence they represent lower limits since the curves scale as $1 + R$. The first of these behaviours would make some difference to the determination of $\Delta\Sigma$ so its exclusion removes a significant uncertainty.

Data with impressive statistical precision were also shown by Hermes¹⁷ and E155¹⁸. The collaborations have not yet evaluated the first moments over the full x range but this will be done soon so that we shall have more precise tests of QCD via the Bjorken sum rule and improved measurements of $\Delta\Sigma$.

2.2 Measurements of Δu_V , Δd_V and $\Delta\bar{q}$ using inclusive hadrons

These quantities were derived by both HERMES and the SMC from the observed distributions of events in polarised DIS in which final state hadrons were observed^{17,19}. This method assumes factorisation in the quark parton model and measured values of the fragmentation functions. The integrals over the observed quark distributions are consistent with those obtained from the structure function measurements. We look forward in the future to more precise measurements of these quantities. In section 4, we will return to the use of semi-inclusive measurements as a way to measure the gluon polarization. Such measurements will probably be needed to determine how the nucleon's spin is shared between ΔG and L .

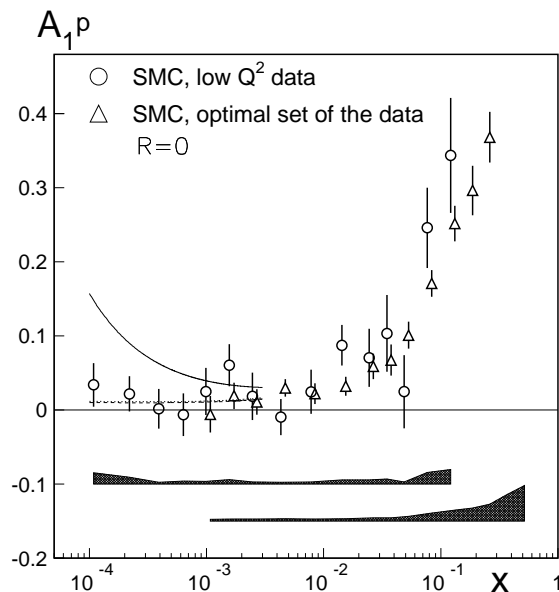


Figure 2: The values of A_1^p as a function of x measured by SMC¹⁶. The smooth curves show the expected behaviour of A_1^p as $x \rightarrow 0$ proposed in⁷. The solid curve shows the behaviour for $g_1^p \sim 1/x \ln^2 x$, the dashed curve for $g_1 \sim \ln x$ and the dotted curve $g_1 \sim (2 + \ln x)$.

2.3 g_2 measurements

E155 presented measurements²⁰ of g_2 which show consistency with the Burkhardt-Cottingham sum rule²¹ and with earlier SMC data²². These measurements show that g_2 is small. Hence it causes little systematic error in the determination of g_1 . The data reported came from a short run at SLAC. A longer run which will allow much improved precision is planned for next year. We will return to the relevance of g_2 in section 5.2.

3 Theoretical aspects of polarized DIS

Next, we turn to some theoretical aspects that are important to understand in more detail the results in polarized DIS. Within the framework of QCD, one finds that a generic cross section or structure function $F(x, Q^2)$ can be written

as a convolution

$$F(x, Q^2) = \sum_i \int dy dz \delta(x - yz) C_i(y, Q^2/\mu^2, \alpha_s) q_i(y, \mu^2), \quad (7)$$

where $q_i(y, \mu^2)$ are quark distribution functions at a given scale (the soft part) and $C_i(y, Q^2/\mu^2, \alpha_s)$ are coefficient functions (the hard part) calculable in perturbative QCD. By taking moments of the structure functions, e.g. the lowest moment $\Gamma(Q^2) = \int_0^1 dx F(x, Q^2)$ one arrives at

$$\Gamma(Q^2) = \sum_i C_i(Q^2/\mu^2, \alpha_s) q_i(\mu^2), \quad (8)$$

which relates the moments of structure functions via calculable coefficient functions $C_i(Q^2/\mu^2, \alpha_s)$ to moments of quark distributions, which can be expressed as scale dependent matrix elements $q_i(\mu^2)$ of quark and gluon matrix elements between proton states. In Eq. 4 we have already seen the above relation at leading order, α_s^0 , relating the first moment of $g_1(x, Q^2)$ to axial matrix elements Δq or the combinations a_i . The ‘QCD-improved’ result is given by

$$\begin{aligned} \Gamma_1^{p(n)}(Q^2) = & +(-)\frac{1}{12} C_{NS} \underbrace{(\Delta u - \Delta d)}_{a_3(\not{\mu}^2)} + \frac{1}{36} C_{NS} \underbrace{(\Delta u + \Delta d - 2\Delta s)}_{a_8(\not{\mu}^2)} \\ & + \frac{1}{9} C_S \underbrace{(\Delta u + \Delta d + \Delta s)}_{\Delta\Sigma(\mu^2)=a_0(\mu^2)} \end{aligned} \quad (9)$$

(\overline{MS} scheme), where $\not{\mu}^2$ indicates that the matrix element is scale-independent. At order α_s^1 (NLO) the coefficient functions $C_S = 1 - \alpha_s/3\pi + \dots$ and $C_{NS} = 1 - \alpha_s/\pi + \dots$ and the next terms become scheme-dependent. The non-singlet matrix elements are scale-independent, but as a consequence of the nonconservation of the singlet axial current through the Adler-Bell-Jackiw anomaly, the matrix element $\Delta\Sigma = a_0$, and hence also the Δq ’s separately, are scale-dependent. Including a gluonic contribution in a redefinition of the matrix elements (distribution functions and their moments) one can define scale-independent quantities

$$\Delta\tilde{q}(\not{\mu}^2) = \Delta\tilde{q}(\mu^2) + \frac{\alpha_s}{2\pi} \Delta G(\mu^2), \quad (10)$$

in which case one has

$$\begin{aligned} \Gamma_1^{p(n)}(Q^2) = & +(-)\frac{1}{12} C_{NS} \tilde{a}_3(\not{\mu}^2) + \frac{1}{36} C_{NS} \tilde{a}_8(\not{\mu}^2) \\ & + \frac{1}{9} C_S \Delta\tilde{\Sigma}(\not{\mu}^2) + n_f C_G \frac{\alpha_s}{2\pi} \Delta G(\mu^2) \end{aligned} \quad (11)$$

Table 1: Values for the scale-independent quark spin contributions $\Delta\tilde{q}$ (see Eq. 10) for different scenarios for the strange quark matrix element $\Delta\tilde{s}$. Quantities in parentheses are fixed by experiments.

Quantity	Scenario I	Scenario II	Scenario III
$\Delta\tilde{u}(\mu^2)$	+0.92	+0.87	+0.82
$\Delta\tilde{d}(\mu^2)$	-0.34	-0.39	-0.44
$\Delta\tilde{s}(\mu^2)$	-0.00	-0.05	-0.10
$a_3(\mu^2)$	(1.26)	(1.26)	(1.26)
$a_8(\mu^2)$	(0.58)	(0.58)	(0.58)
$\Delta\Sigma(\mu^2)$	0.58	0.43	0.28
$\Delta\Sigma(10\text{ GeV}^2)$	(0.25)	(0.25)	(0.25)
$\Delta G(10\text{ GeV}^2)$	2.8	1.5	0.3

(Adler-Bardeen scheme). The result for $\Gamma_1^p - \Gamma_1^n$ (Bjorken sum rule) only involves scale-independent matrix elements. It only receives QCD corrections via the calculable coefficients C_{NS} , which multiplies the result given in Eq. 6. This coefficient is now known¹³ up to α_s^3 , with estimates¹⁴ for the next order and the calculations agree with experiment (see section 1, Fig. 1). The values of Γ_1^p and Γ_1^n each contain the scale-dependent matrix element $\Delta\Sigma(\mu^2)$ or $\alpha_s \Delta G(\mu^2)$ and hence they are useful as measurements to determine this matrix element, but they should no longer be referred to as sum rules²⁵.

The most modern values of a_3 and a_8 are 1.260²³ and 0.575²⁴, respectively. Taken with $\Delta\Sigma(10\text{ GeV}^2) \approx 0.25$, extracted from the measurements of Γ_1^p and/or Γ_1^n , this gives us three pieces of data to learn about the quantities appearing in Eqs. 9 or 11. Three scenarios are sketched in which each differs in the value of $\Delta\tilde{s}$, the scale-independent strange quark spin contribution. Choosing $\Delta\tilde{s} \equiv 0.00, -0.05$ and -0.10 respectively, one sees in Table 1 what this implies for the scale-dependent polarized gluon distribution, assuming $\alpha_s(10\text{ GeV}^2) \approx 0.25$. The strong variation of $\Delta G(10\text{ GeV}^2)$ shows the insensitivity of inclusive DIS for this quantity. The results of a more elaborate analysis for the polarized quark and gluon distributions in both the \overline{MS} and AB schemes were presented in the talk by Sichtermann²⁹. Using the different schemes, the results (omitting systematic errors) for ΔG were found to be

$$\Delta G(5\text{ GeV}^2) = 0.25^{+0.29}_{-0.22} \quad (\overline{MS} \text{ scheme}) \quad (12)$$

$$\Delta G(5\text{ GeV}^2) = 0.99^{+1.17}_{-0.31} \quad (\text{AB scheme}) \quad (13)$$

This illustrates the insensitivity of inclusive DIS to the polarized gluon dis-

tribution. If in a more precise analysis of this type the scheme dependence persists it will be an indication that NNLO effects need to be included in this type of analysis. We also note that at this stage of refinement, i.e. incorporating DGLAP evolution, approximations such as $A_1(x, Q^2) \approx A_1(x)$ should not be used in the data analysis (see also Ref. ²⁶).

Returning to the spin of the nucleon and the sum rule $1/2 = 1/2 \Delta\Sigma + \Delta G + L_q + L_G$, we see that the inclusive analysis shows us the importance of an *independent* measurement of ΔG . Furthermore, we know that $\Delta G(Q^2) \propto 1/\alpha_s(Q^2)$ and so it grows with increasing Q^2 . This points to the importance of measuring the orbital contribution to the angular momentum²⁷ as well as ΔG . One possibility for this which is being investigated is to use virtual Compton scattering²⁸ ($\gamma^* + p \rightarrow \gamma + p'$). However, the cross section for such an exclusive process is rather small.

4 Plans to measure ΔG

In inclusive DIS, the measurements of the polarized gluon distribution is indirect. It enters via the evolution equations, as discussed in the previous section. Only a wide Q^2 range of the data could improve our knowledge of ΔG , possibly requiring theoretical efforts to go to sufficiently high order if the problem of the scheme dependence of the NLO QCD persists²⁹. The option of a future polarized $\vec{e}\vec{p}$ HERA collider, which requires the polarization of protons in the HERA ring, would provide an excellent opportunity for such a measurement³⁰.

A more direct way to measure the gluon distribution is the photon-gluon fusion process, $\gamma^* + G \rightarrow q\bar{q}$. This is planned in the HERMES experiment¹⁷ via the fusion into a $c\bar{c}$ pair, which is reconstructed from the decay of charmed mesons in the final state. Rather than determining the sum rule the experiment is sensitive to $\Delta G(x)/G(x)$ at $x \approx 0.3$. This approach is also proposed by the COMPASS³¹ experiment, which is sensitive to $\Delta G(x)/G(x)$ at $x \approx 0.1$. Another option to obtain the polarized gluon distribution is being studied by COMPASS. This consists of detecting the production of a light $q\bar{q}$ pair from photon-gluon fusion via tagging of an oppositely charged pair of hadrons with large transverse momentum. At a future polarized HERA collider the photon-gluon fusion into a pair of jets is the obvious final state tag. This would give access to $\Delta G(x)$ for $x \leq 0.0015$. A complication in this case is the Compton process $\gamma^* + q \rightarrow q + G$, which also leads to a two jet final state. Important to note is the existence of the calculations of the NLO QCD corrections for charm production, reported at this meeting³².

Hadron induced processes at RHIC³³ and HERA- \vec{N} , the option using polarized protons in HERA in combination with a gas jet target³⁰ were also dis-

cussed at this meeting. On the theoretical side, experimentalists were warned of other possible small- x complications besides the effects of gluons^{34,35}.

5 Unravelling the nucleon structure

5.1 Nonlocal quark and gluon operators

The moments of structure functions are related via the operator product expansion to local quark and gluon operator combinations. The x -dependent quark and gluon distributions themselves also can be expressed in terms of quark and gluon operators, albeit that they are no longer local. One has for the polarized quark helicity distributions,

$$\Delta q(x) = \int \frac{d\xi^-}{4\pi} e^{i x P^+ \xi^-} \langle P, S | \bar{\psi}(0) \gamma^+ \gamma_5 \psi(\xi) | P, S \rangle \Big|_{\xi^+ = \xi_T = 0}, \quad (14)$$

which is a lightcone correlation function^b, and for the polarized gluon distribution one has

$$x \Delta G(x) = \int \frac{d\xi^-}{4\pi} e^{i x P^+ \xi^-} \langle P, S | F^{+\alpha}(0) \tilde{F}_\alpha^+(\xi) | P, S \rangle \Big|_{\xi^+ = \xi_T = 0}. \quad (15)$$

For instance one immediately recovers the result in Eq. 5 after integrating the above result for $\Delta q(x)$ over x . The knowledge of the quark and gluon distributions as matrix elements enables

- Interpretation of quantities as densities, which requires rewriting in terms of good (“partonic”) components of the quark field, $\psi_+ \equiv 1/2 \gamma^- \gamma^+ \psi$. One has

$$\bar{\psi} \gamma^+ \psi \propto \psi_+^\dagger \psi_+, \quad (16)$$

$$\bar{\psi} \gamma^+ \gamma_5 \psi \propto \psi_{+R}^\dagger \psi_{+R} - \psi_{+L}^\dagger \psi_{+L}, \quad (17)$$

where $\psi_{+R/L} \equiv 1/2 (1 \pm \gamma_5) \psi_+$ are chiral projections.

- Study of scale dependence (evolution). For more details on this we refer to the working group on structure functions.
- Calculation of the distributions. Lattice calculations can be used to obtain local matrix elements. Explicit models for hadrons, such as quark potential models, bag models, etc. in principle can be used, given the structure of the matrix element. A difficulty here is the usual lack of a fully covariant description.

^b $a^\pm = (a^0 \pm a^3)/\sqrt{2}$ are lightcone components

5.2 Higher twist contributions: g_2

The remarks in the previous paragraph are perhaps best illustrated on the example of the distribution $g_T(x) = g_1(x) + g_2(x)$, which is the $1/Q$ -suppressed combination in the asymmetry in Eq. 1. It is connected to “less-trivial” operators than the one in the previous section, in this case

$$S_T^\alpha g_T(x) = \int \frac{d\xi^-}{4\pi} e^{ixP^+\xi^-} \langle P, S | \bar{\psi}(0) \gamma^\alpha \gamma_5 \psi(\xi) | P, S \rangle \Big|_{\xi^+ = \xi_T = 0}, \quad (18)$$

After some massaging, using Lorentz covariance and the QCD equations of motion g_2 can be separated into two parts,

$$g_2(x) = g_2^{WW}(x) + \tilde{g}_2(x), \quad (19)$$

where the first term is the Wandzura-Wilczek contribution³⁶, which can be calculated from g_1 and a so called interaction-dependent part, which involves quark-gluon-quark correlation functions. For g_2 several sum rules exist, the most well-known being the Burkhardt-Cottingham sum rule²¹, $\int dx g_2(x) = 0$, which is also satisfied by the separate terms in the above relation for g_2 . Other sum rules that recently have been studied are the Efremov-Leader-Teryaev sum rule³⁷. The new E155 data, described in section 2.3, show consistency with the Burkhardt-Cottingham sum rule and indicate that $\tilde{g}_2(x)$ is small. In Ref.²⁰ a comparison of the particular moment d_2 with theoretical estimates from models and lattice calculations has been shown.

5.3 Transverse spin distribution: h_1 or $\Delta_T q$

At leading order the soft part governing the quark content of a spin 1/2 hadron can be described with three quark distributions. The most well-known are the unpolarized quark distribution $q(x)$ or $f_1(x)$ and the quark chirality (or helicity) distribution $\Delta q(x)$ or $g_1(x)$, involving the operator structures in Eqs. 16 and 17 respectively. The third one is the quark transverse spin distribution $\Delta_T q(x)$ or $h_1(x)$. While $g_1(x)$ involves chiral projections $\psi_{+R/L}$ of the quark field, the function $h_1(x)$ contains the following quark operators,

$$\bar{\psi} \gamma^1 \gamma^+ \psi \propto \psi_{+\uparrow}^\dagger \psi_{+\uparrow} - \psi_{+\downarrow}^\dagger \psi_{+\downarrow}, \quad (20)$$

where $\psi_{+\uparrow/\downarrow} \equiv 1/2 (1 \pm \gamma^1 \gamma_5) \psi_+$ are transverse spin projections. It requires a transversely polarized nucleon to measure this function. Rewritten in terms of chiral quark fields, the operator structure is $\psi_{+R}^\dagger \psi_{+L}$, hence the soft part requires a chirality flip and the function is referred to as *chirally odd*. In

hard processes, this can only be achieved by a nonzero quark mass, hence the function is suppressed in inclusive deep inelastic scattering. In semi-inclusive processes, it is possible to combine two soft chirally odd parts, the first describing the quark content of the target and the second describing the quark fragmentation into hadrons. We mention two possibilities,

- Drell-Yan scattering³⁸, where the asymmetry³⁹

$$A_{TT} \propto \sum_a h_1^a(x_A) h_1^{\bar{a}}(x_B), \quad (21)$$

is sensitive to annihilating transversely polarized quarks in the scattering of two transversely polarized nucleons.

- Semi-inclusive DIS, where one can consider spin transfer from a transversely polarized nucleon via a transversely polarized quark to a transversely polarized hadron in the final state, e.g. the process⁴⁰ $ep^\uparrow \rightarrow e\Lambda^\uparrow X$. Another possibility⁴¹ is to use azimuthal asymmetries in semi-inclusive DIS, e.g.

$$\langle \sin(\phi_h^\ell + \phi_S^\ell) \rangle_{OT} \propto \sum_a h_1^a(x) H_1^{\perp(1)a}(z), \quad (22)$$

where the function $H_1^{\perp(1)a}(z)$ is a fragmentation function into an unpolarized or spinless final state, which correlates the quark transverse spin to the transverse momentum relative to the produced hadron. In this way it leads to an azimuthal asymmetry involving the azimuthal angles ϕ_h^ℓ and ϕ_S^ℓ of a produced hadron or a target spin relative to the lepton scattering plane^{42,43}.

The evolution of these functions is known and is different from that of the helicity distributions³⁸.

6 Conclusion

Several other items have been discussed in the spin working group. We have just mention the detailed investigation of the effects of transverse quark momenta in various hard processes such as Drell-Yan scattering, semi-inclusive DIS and e^+e^- annihilation^{41,43,44}, the quark distributions in higher spin targets and their sensitivity to specific correlations in the target, e.g. the presence of pionic components⁴⁵. We also mention the possibilities to use polarization to zoom in on new phenomena³⁰, e.g. to decide on contact interactions proposed⁴⁶ to explain the possible excess of high Q^2 events at HERA, or to

improve our knowledge of the polarized quark distributions via charged current interactions. Both of these are examples of new possibilities offered by polarized protons in HERA. This also offers possibilities to study spin effects in diffractive processes⁴⁷ or to study the polarized quark distributions in the photon⁴⁸.

Returning to the present, at this meeting we have seen measurements of impressive precision of the polarised structure functions g_1 and g_2 of the proton and neutron. We look forward to further data in the future. Evidence has been presented in the workshop which shows that the observed deficiency of the spin of the nucleon carried by the quarks is not due to perverse Regge behaviour which affects the extrapolation to small x . Hence the problem of the distribution of the nucleon's spin still persists. It is still not possible to say whether the deficiency of the nucleon's spin carried by the quarks is taken up by ΔG or L and theoretical refinements will be required here to understand the scheme dependence of the QCD fits to the data. We look forward to future experiments (e.g. HERMES, Compass, RHIC, E156, HERA) which will make direct determinations of ΔG .

Acknowledgments

We thank the organisers for creating such an interesting, stimulating and enjoyable workshop. We also thank all the participants in Working Group 4 for their assistance in preparing this talk. We are grateful to R G Roberts for valuable discussion.

References

1. V W Hughes and J Kuti; Ann.Rev.Nucl.Part.Sci 33 (1983) 611.
2. SLAC E80,M J Alguard et al; Phys. Rev. Lett. 37 (1976) 1261. SLAC E130,G Baum et al; Phys. Rev. Lett. 51 (1983) 1135.
3. EMC, J Ashman et al, Phys. Lett. B206 (1988) 364 and Nucl. Phys. B328 (1989) 1
4. A V Efremov and O V Teryaev, Czech.Hadron Symp. (1988)302.
5. G Altarelli and G G Ross; Phys. Lett. B212 (1988) 391.
6. S J Brodsky J Ellis and M Karliner; Phys. Lett. B206 (1988) 309.
7. F E Close and R G Roberts; Phys. Lett. B336 (1994) 1257.
8. J Bartels, B I Ermolaev and M G Ryskin; Z.Phys. C72 (1996) 627.
9. SMC D.Adams et al; Phys. Lett. B329 (1994) 399.
10. SLAC-E142, D L Anthony et al; Phys. Rev. Lett. 71 (1993) 959. SLAC-E143, K Abe et al; Phys. Rev. Lett. 74 (1995) 346.
11. J D Bjorken, Phys. Rev. 179 (1969) 1547.

12. R P Feynman, *Photon-Hadron Interactions* (Benjamin Press, 1972)
13. J. Kodaira et al Phys. Rev. D20 (1979) 627. S A Larin, F V Tkachev and J A M Vermaseren, Phys. Lett. B259 (1991) 345. S A Larin and J A M Vermaseren, Phys. Rev. Lett. 66 (1991) 862.
14. A.L.Kataev and V Starshenko Mod. Phys. Lett. A10 (1995) 235.
15. SMC, Talk by J Cranshaw, these proceedings.
16. SMC, Talk by J Kiryluk, these proceedings.
17. HERMES, Talk by K Rith, these proceedings.
18. E155, Talk by H Borel, these proceedings.
19. SMC, Talk by A Sandacz, these proceedings.
20. Talk by S Rock, these proceedings.
21. H Burkhardt and W N Cottingham, Ann. Phys. (N.Y.) 56 (1970) 453.
22. SMC, D Adams et al; Phys. Lett. B336 (1994) 125.
23. Particle Data Table Phys. Rev. D54 (1996)
24. F E Close and R G Roberts Phys.Lett. B316 (1993) 165.
25. J Ellis and R L Jaffe, Phys. Rev. D9 (1974) 1444.
26. Talk by A Kotikov, these proceedings.
27. X Ji, J Tang and P Hoodbhoy, Phys. Rev. Lett. 76 (1996) 740.
28. A V Radyushkin, Phys. Lett. B380 (1996) 417; X Ji, in Proceedings of the 12th International Symposium on High-energy Spin Physics, Amsterdam, 10-14 Sep 1996, C W de Jager et al. (ed), p. 68; X Ji and J Osborne, Phys. Rev. D57 (1998) 1337.
29. SMC, Talk by E Sichtermann, these proceedings; G. Altarelli, R.D. Ball, S. Forte and G. Ridolfi, Nucl. Phys. B496 (1997) 337.
30. Talk by G Radel, these proceedings.
31. Talk by G Mallot, these proceedings.
32. Talk by M Stratmann, these proceedings.
33. Talk by N Hayashi, these proceedings.
34. Talk by B Badelek, these proceedings.
35. Talk by N Kochelev, these proceedings.
36. S Wandzura and F Wilczek, Phys. Lett. B72 (1977) 195.
37. A V Efremov, O V Teryaev and E Leader, Phys. Rev. D55 (1997) 4307.
38. Talk by S Kumano, these proceedings.
39. R L Jaffe and X Ji, Nucl. Phys. B375 (1992) 527.
40. X Artru and M Mekhfi, Z. Phys. 45 (1990) 669; X Artru and M Mekhfi, Nucl. Phys. A532 (1991) 351C.
41. Talk by R Jakob, these proceedings.
42. J Collins, Nucl. Phys. B396 (1993) 169.
43. P J Mulders and R D Tangerman, Nucl Phys B461 (1996) 197
44. R D Tangerman and P J Mulders, Phys Rev D51 (1995) 3357; D Boer,

- R Jakob and P J Mulders, Nucl Phys B504 (1997) 345.
- 45. Talk by W Schaefer, these proceedings.
 - 46. J M Virey, hep-ph/9710423.
 - 47. Talk by B Kopeliovich, these proceedings.
 - 48. Talk by T Gehrmann, these proceedings.